Closing the hierarchy of moment equations in nonlinear dynamical systems

C. Nicolis
Institut Royal Météorologique de Belgique, Avenue Circulaire 3, 1180 Brussels, Belgium

G. Nicolis
Center for Nonlinear Phenomena and Complex Systems, Université Libre de Bruxelles, Campus Plaine, Code Postal 231, 1050 Brussels, Belgium

(Received 3 April 1998)

The moment equations associated with the evolution of the probability density are known to form an infinite hierarchy of coupled equations in nonlinear dynamical systems. In the present paper a systematic approach for closing this hierarchy is proposed, based on the ansatz that in the long time limit there exist groups of moments varying on the same time scale. The method is applied to a one-dimensional vector field in the presence of noise, and to two prototypes of chaotic behavior. Excellent agreement with numerical results is obtained. Special emphasis is placed on the role of symmetries, and on the origin of the composite oscillations found for certain types of moments in the chaotic systems. [S1063-651X(98)01310-5]

PACS number(s): 05.45.+b, 05.40.+j

I. INTRODUCTION

It is widely recognized that the probabilistic description constitutes the natural mode of approach to large classes of dynamical systems. On the one hand, such systems are often subjected to a variety of forcings, including the internally generated thermodynamic fluctuations, which can in certain cases be assimilated to a stochastic process, thereby eliciting a response at the level of the system's observables which can best be described in probabilistic terms [1]. On the other hand, as well known, purely deterministic systems obeying nonlinear evolution laws can generate complex behavior in the form of multiple solutions or aperiodic space-time evolutions, of which deterministic chaos is the most striking example [2]. Under these conditions the state of the system becomes markedly delocalized in phase space, and, once again, the probabilistic description offers the most natural way to account for this variability and to characterize it in terms of quantities related to the intrinsic properties of the underlying dynamics [2,3]. This approach has been used successfully in, among others, the problem of prediction in the context of atmospheric and climate dynamics [4], and the characterization of multifractals [5] and fully developed turbulence [6].

A typical feature of the probabilistic description is to express the evolution of probability densities in terms of a *linear* evolution equation, as opposed to the generally nonlinear character of the corresponding deterministic description. Furthermore, while in a nonlinear system the deterministic description may predict a variety of instabilities, in the probabilistic system the probability density will be driven irreversibly to a final invariant state, as long as the system enjoys sufficiently strong ergodic properties. The complexity of the deterministic nonlinear dynamics will show up, then, through the nonlinear dependence of the coefficients of the evolution equations of the probability densities in the phase space variables. As a result of this, it is generally not possible to find closed-form solutions for such densities.

On the other hand, typical macroscopic observables associated with a system are generally low-order moments of the probability density. To characterize the macroscopic state of such a system, it would therefore suffice to compute these first few moments instead of the full density function. It is here that one encounters a ubiquitous limitation, complicating, at the outset, the probabilistic study of nonlinear systems: owing to the nonlinear dependence of the coefficients of the equation for the probability density, the low-order moments do not obey closed evolution equations but are, rather, linked to the high-order ones by an infinite *hierarchy* of coupled equations.

Several attempts at overcoming this fundamental difficulty have been reported in the literature. The first idea that comes to mind is to neglect higher order moments or, more precisely, the corresponding variances or cumulants, altogether. This gives reasonable results in systems operating around a stable steady state and submitted to weak noise, but fails completely in the presence of strong fluctuations and/or chaotic dynamics. A somewhat related technique, subject essentially to the same limitations, is to linearize the coefficients of the equations for the probability densities around a reference state [1]. A third type of approach consists of seeking for scaling relations between moments, using arguments inspired by Kolmogorov's theory of turbulence [6]. It has been applied recently both at the level of heuristic models [7] and at the level of the Navier-Stokes equations [8]. The objective of the present paper is to propose a systematic approach to the truncation of the moment hierarchies, and to apply it to representative case studies.

The main idea, presented in Sec. II, is to express high-order moments as time-independent functionals of the low-order ones. This stems from the observation that in the regime of long (but not infinite) times there exist subclasses of moments varying on the same time scale, given by the dominant eigenvalue(s) of the evolution operator for the probability density. This provides, then, a natural closure scheme linking the high-order moments to the first few ones. As a preliminary exercise, in Sec. III a deterministic one-dimensional vector field is considered, and shown not to sat-

isfy the ansatz of Sec. II, owing to the quasi-independent evolution of the successive moments. Section IV is devoted to a study of this system in the presence of noise. It is shown that noise provides the kind of coupling needed to synchronize the moments, thereby allowing for closed-form equations for the evolution of the mean value and the second moment. This result is fully corroborated by numerical experiments.

The case of chaotic dynamics is considered in Secs. V and VI dealing, successively, with the Rössler and the Lorenz models. Closure is again shown to hold true, and the intricate role of symmetries in the evolution equations is brought out. The main conclusions are finally drawn in Sec. VII.

II. FORMULATION

In the sequel we shall be dealing with dynamical systems obeying deterministic evolution laws of the form

$$\frac{d\mathbf{x}}{dt}=\mathbf{F}(\mathbf{x},\mu), \tag{1a}$$

or with systems subjected, in addition, to a stochastic forcing reflecting environmental or internal variability,

$$\frac{d\mathbf{x}}{dt}=\mathbf{F}(\mathbf{x},\mu)+\mathbf{R}(t). \tag{1b}$$

Here $\mathbf{x}=(x_1,\ldots,x_n)$ is the set of variables, $\mathbf{F}=(F_1,\ldots,F_n)$ the evolution laws, μ stands for the control parameters, and $\mathbf{R}(t)$ denotes the random force. We shall limit ourselves to the case where $\mathbf{R}(t)$ is an additive Gaussian white noise,

$$\begin{aligned}\langle\mathbf{R}(t)\rangle&=0,\\ \langle R_i(t)R_j(t')\rangle&=D_{ij}\delta(t-t'),\end{aligned} \tag{2}$$

where it is understood that the covariance matrix $\{D_{ij}\}$ is positive definite.

The evolution of the probability densities associated with Eqs. (1a) and (1b) is given, respectively, by the Liouville and the Fokker-Planck equations [1–3],

$$\frac{\partial\rho}{\partial t}=-\sum_i\ \frac{\partial}{\partial x_i}F_i\rho\equiv\hat{L}\rho\ \ \text{(Liouville equation)}, \tag{3a}$$

$$\begin{aligned}\frac{\partial\rho}{\partial t}&=-\sum_i\ \frac{\partial}{\partial x_i}F_i\rho+\frac{1}{2}\sum_{ij}\ D_{ij}\frac{\partial^2\rho}{\partial x_i\partial x_j}\\ &\equiv\hat{P}\rho\ \ \text{(Fokker-Planck equation)}.\end{aligned} \tag{3b}$$

We define the set of kth-order moments of ρ as follows:

$$\begin{aligned}m_{k_1\cdots k_n}(t)=\overline{x_1^{k_1}\cdots x_n^{k_n}}&=\int dx_1\cdots dx_n x_1^{k_1}\cdots x_n^{k_n}\rho(x_1,\cdots x_n,t)\\ k_1+\cdots+k_n&=k.\end{aligned} \tag{4a}$$

Multiplying both sides of Eqs. (3a) and (3b) by $x_1^{k_1}\cdots x_n^{k_n}$, integrating over phase space and performing integrations by parts (being understood that ρ tends rapidly to zero as $|\mathbf{x}|\to\infty$) one obtains, respectively,

$$\frac{d}{dt}\overline{x_1^{k_1}\cdots x_n^{k_n}}=\sum_i\ k_i\overline{x_1^{k_1}\cdots x_i^{k_i-1}\cdots x_n^{k_n}F_i} \tag{4b}$$

and

$$\begin{aligned}\frac{d}{dt}\overline{x_1^{k_1}\cdots x_n^{k_n}}&=\sum_i\ k_i\overline{x_1^{k_1}\cdots x_i^{k_i-1}\cdots x_n^{k_n}F_i}\\ &\quad+\tfrac{1}{2}\sum_{ij}\ D_{ij}k_ik_j\overline{x_1^{k_1}\cdots x_i^{k_i-1}\cdots x_j^{k_j-1}x_n^{k_n}}.\end{aligned} \tag{4c}$$

We see that, as anticipated in Sec. I, as long as F_i is not linear in x_i, Eqs. (4b) and (4c) indeed constitute infinite hierarchies of equations linking moments of order k to moments of at least order $k+1$. On the other hand, the second term in Eq. (4c) introduces a moment of order $k-2$. As we see later, this term will be responsible for the coupling of all moments and their eventual synchronization to the same time scale.

Let $\{\lambda_n\}$, $n=0,1...$, be the eigenvalues of $\hat{L}$ or $\hat{P}$. To express the main idea of this paper in as simple a setting as possible, we assume $\{\lambda_n\}$, $n\neq0$, to be discrete, nondegenerate, and separated from the invariant eigenvalue $\lambda_0=0$ by a *finite* gap. Furthermore, we consider systems having sufficiently strong ergodic properties, so that a typical initial condition $\rho_0(\mathbf{x})$ is driven irreversibly to the invariant distribution $\rho_s(\mathbf{x})$. This implies that

$$\text{Re}\ \lambda_n<0,\quad n\neq0. \tag{5}$$

By ordering the λ_n's according to increasing absolute values of their real parts we may then write formally the solution of Eqs. (3a) or (3b) as

$$\delta\rho_t(\mathbf{x})=\rho_t(\mathbf{x})-\rho_s(\mathbf{x})=\sum_{n=1}^{\infty}C_ne^{\lambda_nt}\phi_n, \tag{6}$$

where $\{\phi_n\}$ are the right eigenfunctions of the operator, and the expansion coefficients $\{C_n\}$ are given by

$$C_n=(\tilde{\phi}_n,\rho_0)=\int d\mathbf{x}\ \tilde{\phi}_n(x)\rho_0(\mathbf{x}). \tag{7a}$$

Here $\tilde{\phi}$ are the left eigenfunctions, and we have used the biorthogonality relation

$$(\tilde{\phi}_n,\phi_n)=\delta_{nn'}^{kr}. \tag{7b}$$

Notice that $\phi_0=\rho_s$ and $\tilde{\phi}_0=1$.

The deviation of the kth-order moment from its asymptotic value is given by integrating the *vector monomial*

$$\mathbf{x}^k=x_1^{k_1}\cdots x_n^{k_n},\quad k_1+\cdots+k_n=k$$

over $\delta\rho_t(\mathbf{x})$:

$$\delta\overline{\mathbf{x}^k}=\sum_{n=1}^{\infty}C_ne^{\lambda_nt}(\mathbf{x}^k,\phi_n)=\sum_{n=1}^{\infty}C_ne^{\lambda_nt}\mathbf{B}_{kn}. \tag{8}$$

Equations (6) and (8) imply that in the limit of long times $\delta\rho_t$ and its moments will be dominated by the eigenvalues λ_n having the smallest real parts. Let $\lambda_1,\ldots,\lambda_s$ be the set of such eigenvalues. We then have, from Eq. (8),

$$\delta\overline{\mathbf{x}^k} \approx \sum_{n=1}^{s} C_n e^{\lambda_n t}\mathbf{B}_{kn}, \quad 1 \leqslant k \leqslant s. \tag{9}$$

These relations can be viewed as a system of equations linking $C_n e^{\lambda_n t}$ to $\delta\overline{\mathbf{x}^k}$ through the inverse matrix $\mathbf{B}^{-1}$ of $\{\mathbf{B}_{kn}\}$,

$$\begin{pmatrix} C_1 e^{\lambda_1 t} \\ \vdots \\ C_s e^{\lambda_s t} \end{pmatrix} = \mathbf{B}^{-1} \begin{pmatrix} \delta\overline{x} \\ \vdots \\ \delta\overline{x^k} \end{pmatrix}. \tag{10}$$

Now let $\delta\overline{\mathbf{x}^m}$, $m > s$, be a higher order moment. According to Eqs. (9) and (10),

$$\delta\overline{\mathbf{x}^m} \approx \sum_{n=1}^{s} C_n e^{\lambda_n t}\mathbf{B}_{mn} = \sum_{n,n'=1}^{s} \mathbf{B}_{mn}(\mathbf{B}^{-1})_{nn'}\delta\overline{\mathbf{x}^{n'}}, \quad m > s. \tag{11}$$

This relation expresses the mth moment $m > s$ as a superposition of s lower order moments. It therefore provides us with a way to close the hierarchy of moment equations to its first s members. The procedure holds true as long as $\mathbf{B}$ is invertible and the $\mathbf{B}_{mn}$'s are not all zero. As we will see shortly, this may indeed happen in the presence of symmetries, in which case the above scheme should be properly amended by restricting the sums to terms having similar symmetry properties.

III. 1D VECTOR FIELD: DETERMINISTIC CASE

In order to gain insight on the necessary ingredients for closure we consider in this section a simple model in which all calculations, including the determination of the full form of the probability density itself, can be carried out explicitly.

We start with the case of a linear one-dimensional (1D) vector field

$$\frac{dx}{dt} = \mu x, \quad \mu < 0, \tag{12}$$

corresponding in the general setting of Eq. (1a) to $F(x) = \mu x$. The moment equations (4b) then read

$$\frac{d\overline{x^k}}{dt} = k\mu\overline{x^k}, \tag{13}$$

showing that moments are decoupled and each of them varies on a different scale, $(k\mu)^{-1}$. This is, therefore, a case where closure is not expected to work.

To see how this shows up in our formulation we consider the Liouville operator associated with Eq. (12),

$$\hat{L} = -\frac{\partial}{\partial x}\,\mu x. \tag{14}$$

The eigenvalues and eigenfunctions of this operator have been fully determined in Ref. [9]. One finds

$$\lambda_n = -n|\mu|,$$

$$\phi_n = (-1)^n \delta^{(n)}(x),$$

$$\tilde{\phi}_n = \frac{\mathbf{x}^n}{n!}, \quad n = 0,1,2,\ldots . \tag{15}$$

The spectral representation of $\delta\rho_t$ and $\delta\overline{x^k}$ in this basis read [Eqs. (6) and (8)]

$$\delta\rho_t(x) = \sum_{n=1}^{\infty} C_n e^{-n|\mu|t}(-1)^n \delta^{(n)}(x),$$

$$\delta\overline{x^k} = \sum_{n=1}^{\infty} C_n e^{-n|\mu|t}(-1)^n \int_{-\infty}^{\infty} dx\; x^k \delta^{(n)}(x). \tag{16a}$$

Using the properties of the Dirac δ function and its derivatives, one sees straightforwardly that

$$B_{kn} = (-1)^n \int_{-\infty}^{\infty} dx\; x^k \delta^{(n)}(x) = 0, \quad k \neq n$$

$$= 1, \quad k = n. \tag{16b}$$

As a result, Eq. (16a) yields

$$\delta\overline{x^k} = C_k e^{-k|\mu|t},$$

in agreement with Eq. (13). Clearly, one is here in the case where either the matrix $\mathbf{B}$ is not invertible or the coupling coefficients $\mathbf{B}_{mn}$ are trivial in Eq. (11).

Next consider a nonlinear vector field with a cubic nonlinearity below the (pitchfork) bifurcation point $\mu = 0$,

$$\frac{dx}{dt} = \mu x - x^3, \quad \mu < 0. \tag{17}$$

The moment equations (4b) are now nonclosed,

$$\frac{d\overline{x^k}}{dt} = k\mu\overline{x^k} - k\overline{x^{k+2}}, \tag{18}$$

but one observes that the (infinite) matrix of coefficients is an upper triangular matrix, suggesting that the moments still vary on different scales. One can confirm this by the study of the spectrum of the Liouville operator corresponding to (17), $\hat{L} = -(\partial/\partial x)(\mu x - x^3)$. One finds [9]

$$x_n = -n|\mu|,$$

$$\phi_n = \frac{\partial}{\partial \xi^n}\,\delta\left[x - \frac{|\mu|^{1/2}\xi}{\sqrt{1-\xi^2}}\right]_{\xi=0}, \tag{19}$$

$$\tilde{\phi}_n = \frac{1}{n!}\left(\frac{x}{\sqrt{x^2+|\mu|}}\right)^n, \quad n = 0,1,2,\ldots .$$

The coefficient B_{kn} in the spectral representation of $\delta\overline{x^k}$, Eq. (8), is thus given by

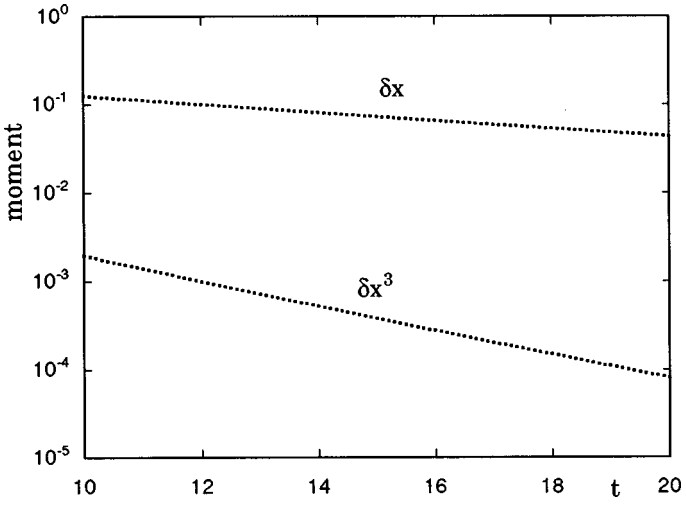

FIG. 1. Long time transient evolution of the first and third excess moments associated with Eq. (17), with $\mu=-0.1$, as obtained from an ensemble of 1000 initial conditions uniformly distributed in the interval $3\leqslant x\leqslant 6$.

$$B_{kn}=\frac{\partial}{\partial\xi^n}\frac{|\mu|^{k/2}\xi^k}{(1-\xi^2)^{k/2}}\bigg|_{\xi=0}.$$

We notice that for $k=1$ one obtains a nonvanishing contribution with $n=1$; for $k=2$ the contribution of B_{21} is zero, and that of B_{22} nonvanishing, etc. We thus recover the separation of the time scales of the linear case, entailing that one cannot expect the existence of closure expressing high-order moments in terms of lower order ones.

We now illustrate these results by means of a numerical experiment, which will also set the stage for similar experiments carried out in the more involved cases of the following sections. Since we want to capture a transient phenomenon (eventually all moments will settle to their asymptotic values if the system has strong ergodic properties), we need to follow the time evolution of an ensemble of phase space points initially far from the asymptotic state ($x=0$ in the present case). To this end, we choose 1000 initial conditions distributed uniformly in the interval [3,6], monitor the instantaneous position of each of these points, and construct the instantaneous values of the various moments by evaluating the discrete analog of Eq. (4a). Figure 1 depicts the result obtained for the first and third moments. We see that the third moment varies three times as fast as the first one, in agreement with the analytical result. This precludes the possibility to express high-order moments as functions of the low-order ones.

IV. 1D STOCHASTICALLY DRIVEN VECTOR FIELD

In this section we consider the effect of noise on the moment dynamics of the nonlinear 1D vector field of Eq. (17). The augmented evolution equation is now [cf. Eq. (1b)]

$$\frac{dx}{dt}=\mu x-x^3+R(t),\quad \mu<0. \tag{20}$$

This gives rise in the white noise limit to a Fokker-Planck equation for the probability density $\rho(x,t)$ of the form [cf. Eq. (3b)]

$$\frac{\partial\rho}{\partial t}=-\frac{\partial}{\partial x}(\mu x-x^3)+\frac{D}{2}\frac{\partial^2\rho}{\partial x^2}, \tag{21}$$

and to the associated moment hierarchy [Eq. (4c)]

$$\frac{d\overline{x^k}}{dt}=\mu k\overline{x^k}-\overline{x^{k+2}}+\frac{1}{2}Dk(k-1)\overline{x^{k-2}},\quad k=1,2,\ldots. \tag{22}$$

As is well known, the eigenfunctions of the Fokker-Planck operator are smooth square integrable functions of x [1,9,10]. In other words the presence of noise, however small, regularizes the highly singular eigenfunctions of the Liouville operator of the previous section appearing in the spectral representation of the excess probability density in Eq. (16a). On the other hand, these new smooth eigenfunctions keep the symmetry of their singular counterparts: odd-indexed ϕ_n's are odd functions of $\mathbf{x}$, and even indexed ϕ_n's are even functions of x. This has an immediate bearing on the spectral representation of the moments [cf. Eqs. (9) and (16a)],

$$\delta\overline{x^k}=\sum_{n=1}^{\infty}C_n e^{\lambda_n t}B_{kn}=\sum_{n=1}^{\infty}C_n e^{\lambda_n t}\int_{-\infty}^{\infty}dx\ x^k\phi_n(x). \tag{23}$$

Specifically, B_{kn} is seen to be zero unless k and n have the same parity. Equation (23) therefore splits into two different sets,

$$\delta\overline{x^{2m}}=\sum_{n\ \text{even}}C_n e^{\lambda_n t}B_{2m,n}, \tag{24a}$$

$$\delta\overline{x^{2m+1}}=\sum_{n\ \text{odd}}C_n e^{\lambda_n t}B_{2m+1,n}. \tag{24b}$$

To proceed further we need some information on the eigenvalues $\{\lambda_n\}$. By mapping Eq. (21) into a Schrödinger-type equation, one can show that the spectrum is discrete and nondegenerate (remembering that $\mu<0$). In the long time limit Eqs. (24) are therefore dominated by the first nontrivial term, which corresponds to $n=2$ in Eq. (24a) and $n=1$ in Eq. (24b). It follows that all even moments and all odd moments taken separately evolve on the same scale, the even moments being faster than the odd ones. This provides us immediately with the necessary ingredients to close the moment hierarchy. To be specific, consider Eq. (22) for $k=1$, written in terms of excess variables around the steady state values,

$$\frac{d\,\delta\overline{x}}{dt}=\mu\,\delta\overline{x}-\delta\overline{x^3}. \tag{25}$$

Now, according to Eq. (24b),

$$\overline{\delta x} \approx C_1 e^{\lambda_1 t} B_{11},$$

$$\overline{\delta x^3} \approx C_1 e^{\lambda_1 t} B_{31} \approx \frac{B_{31}}{B_{11}} \overline{\delta x}, \quad t > \lambda_1^{-1}. \tag{26}$$

Inserting into Eq. (25), one obtains a closed equation for $\overline{\delta x}$,

$$\frac{d\overline{\delta x}}{dt} = \left(\mu - \frac{B_{31}}{B_{11}} \right) \overline{\delta x}. \tag{27}$$

Comparing with Eq. (26), we conclude that $\mu - B_{31}/B_{11}$ is the dominant eigenvalue of the Fokker-Planck operator. B_{31}/B_{11} therefore represents the correction to the Liouvillian eigenvalue $\lambda_1^{(0)} = \mu$ arising from the effect of noise.

Figure 2 describes the result of a numerical evaluation of the first two even and odd moments for $\mu = -0.1$ and $D = 0.01$, obtained by monitoring the time evolution of a nonequilibrium ensemble initially corresponding to a uniform distribution of x in the interval [3,6]. We see that these two sets vary on the same scale, the first being faster than the first second in agreement with the theoretical predictions. To test the closure itself [Eq. (26)], in Fig. 3 we plot the excess third moment $\overline{\delta x^3}$ as a function of $\overline{\delta x}$. We obtain, after an initial time layer, a straight line in agreement with Eq. (26), the slope of which gives the value of the noise correction to the Liouvillian eigenvalue $\lambda_1^{(0)} = -0.1$.

V. CHAOTIC DYNAMICS: ASYMMETRIC CASE

We now turn to higher-dimensional deterministic dynamical systems giving rise to chaotic behavior, focusing first on Rössler-type attractors, which lack any obvious symmetry property. The particular prototype equations we shall consider are [11,12]

$$\frac{dx}{dt} = -y - z,$$

$$\frac{dy}{dt} = x + ay, \tag{28}$$

$$\frac{dz}{dt} = bx - cz + xz.$$

They generate for $a = 0.32$, $b = 0.3$, and $c = 4.5$ weak chaos, whereas for $a = 0.38$, $b = 0.3$, and $c = 4.5$ one obtains a stronger, more mixing form of chaos. We shall refer to these two types of behavior as spiral and screw chaos, respectively.

The complexity of the above dynamics precludes of course any exact result concerning the eigenvalues and eigenfunctions of the Liouvillian, contrary to the case treated in Sec. III. Still, because of the absence of symmetries one expects that in the spectral representation (9) and the closure relations (11) the matrix **B** will be invertible and the expansion coefficients $\mathbf{B}_{mn}$ nonvanishing. As a corollary, and provided that the spectrum remains discrete, all moments should vary on the same time scale, and closure should hold true. This is fully confirmed by numerical experiments to which we turn presently.

Figures 4(a) and 4(b) depict the time evolution of the excess first moments and of three of the six excess second moments in the case of spiral chaos, obtained by using an initial Gaussian ensemble centered on (0,0,0), and having a width equal to the asymptotic values of the second moments. We see that our ansatz is clearly satisfied. The following additional features are also worth noticing (a) that the moments perform composite oscillations in the form of beatings; and (b) the damping of these oscillations remains practically negligible for a substantial period of time, owing presumably to the weak mixing character of spiral chaos. These properties are also shared by other moments as well, such as $\delta \overline{xy}$, etc.

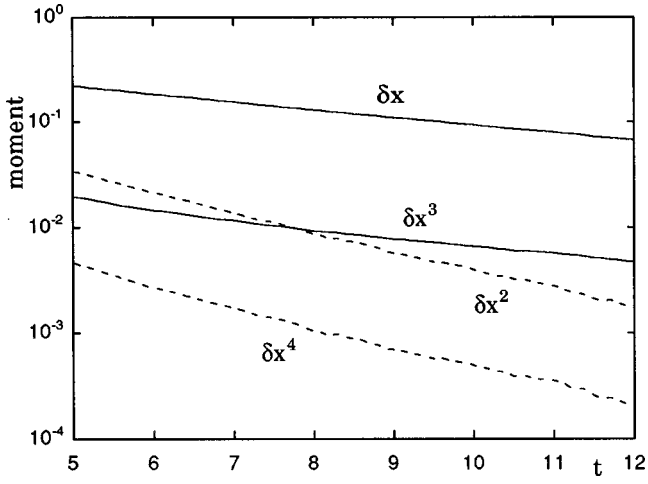

FIG. 2. As in Fig. 1, but for Eq. (20) with $D = 0.01$ and for $\overline{\delta x}$, $\overline{\delta x^3}$ (full line) and $\overline{\delta x^2}$, $\overline{\delta x^4}$ (broken line), as obtained from an ensemble of 20 000 initial conditions.

Figures 5(a) and 5(b) provide the same type of information for the case of screw chaos, again using an initial Gaussian ensemble centered this time on (1,1,1). We again observe composite oscillations, which are now clearly damped.

In the light of the above results a minimal closure would be obtained by overlooking the fast oscillation of frequency ω_f. The dominant eigenvalues of the Liouvillian would then be given by a pair of complex conjugate eigenvalues exhib-

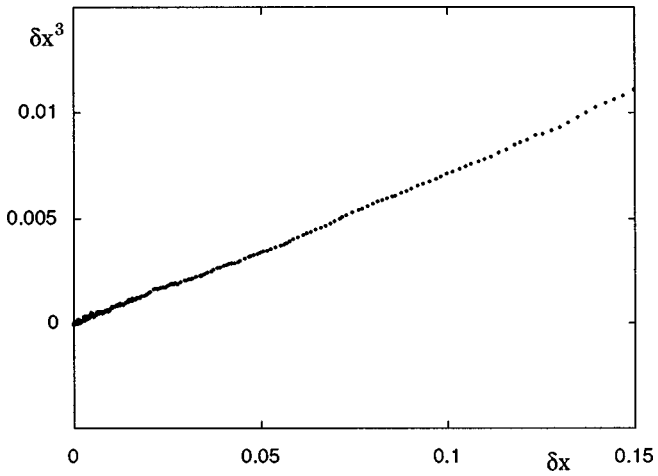

FIG. 3. Dependence of the excess third moment $\overline{\delta x^3}$ on $\overline{\delta x}$ as obtained from the numerical experiment of Fig. 2. The clearcut linear relation provides a justification of the closure relation [Eq. (26)], and gives a noise correction ~0.02 to the Liouvillian eigenvalue.

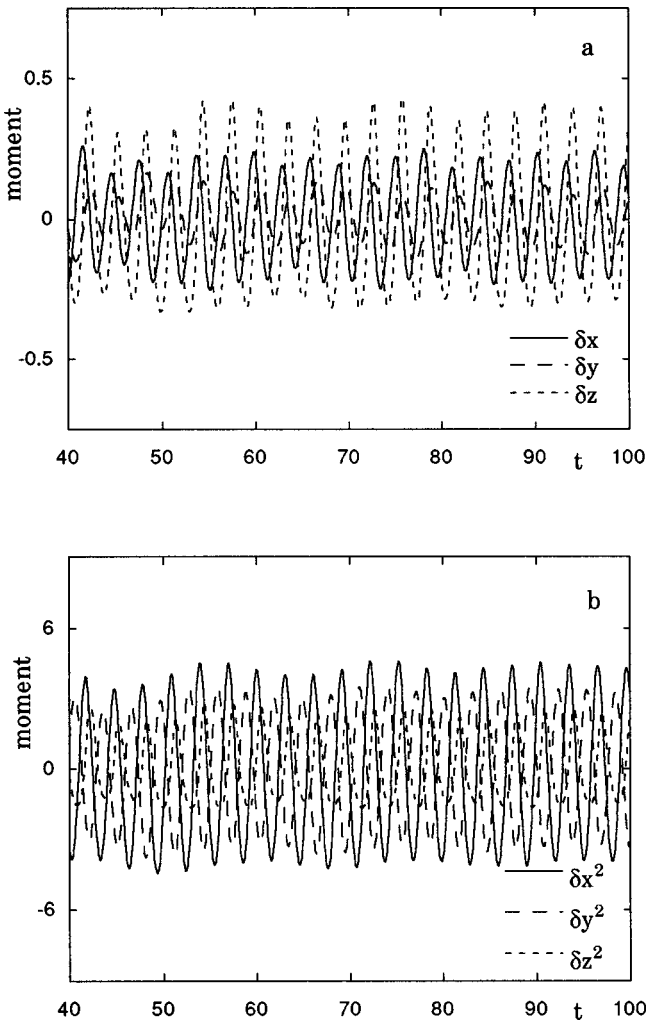

FIG. 4. Long time evolution of $\delta\overline{x}$, $\delta\overline{y}$, and $\delta\overline{z}$ (a), and $\delta\overline{x^2}$, $\delta\overline{y^2}$, and $\delta\overline{z^2}$ (b), in the case of spiral chaos [Eqs. (28) with $a=0.32$, $b=0.3$, and $c=4.5$] as obtained from 20 000 initial conditions distributed according to a Gaussian ensemble centered on (0,0,0) and having a width equal to the asymptotic values of the second moments $\overline{x^2}$, $\overline{y^2}$, $\overline{z^2}$.

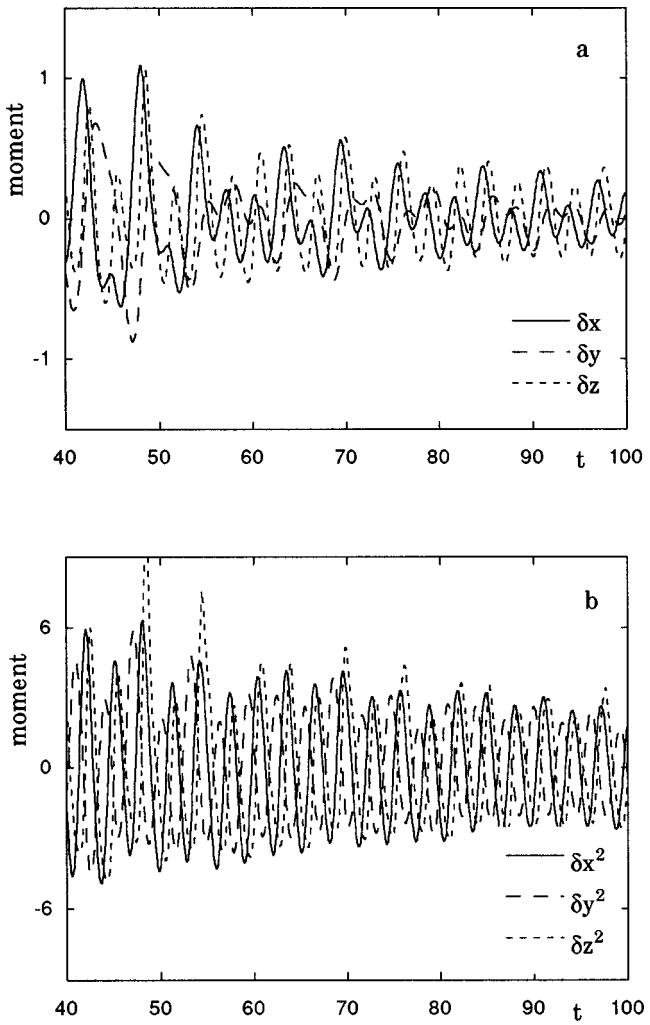

FIG. 5. As in Fig. 4, but in the case of screw chaos [Eqs. (28) with $a=0.38$] and the initial Gaussian ensemble centered on (1,1,1).

iting an imaginary part equal to the slow oscillation frequency ω_s, $\lambda_{1,2}=\mu\pm i\omega_s$. According to Eqs. (9)–(11), this implies that all moments can be expressed in terms of two low-order ones, say $\overline{x}$ and $\overline{y}$. Writing, for instance,

$$\overline{z}=m_1\overline{x}+m_2\overline{y}, \tag{29}$$

and averaging the first two equations (28) one obtains the closed set

$$\frac{d\overline{x}}{dt}=-m_1\overline{x}-(1+m_2)\overline{y}, \tag{30a}$$

$$\frac{d\overline{y}}{dt}=\overline{x}+a\overline{y},$$

whose characteristic equation reads

$$\omega^2+(a-m_1)\omega+1+m_2-m_1a=0. \tag{30b}$$

Requiring that the solutions of this equation reproduce the observed frequency and damping values, one may infer m_1 and m_2, which in this context play a role similar to that of friction coefficients in a damped oscillator. We do not carry this argument further here, postponing a more comprehensive analysis to Sec. VI, dealing with the Lorenz model.

To obtain a more satisfactory closure one needs to account for both the fast and slow oscillations. Now, the time series of Figs. 4 and 5 can be well represented by a function of the form $Ae^{-\mu t}\cos\omega_s t\cos\omega_f t$, where $\cos\omega_s t$ accounts for the amplitude modulation. On the other hand, in the spectral representation of Eq. (9), the time dependencies enter in an additive fashion. One must therefore decompose the above function as

$$Ae^{-\mu t}[\cos(\omega_s-\omega_f)t+\cos(\omega_s+\omega_f)t], \tag{31}$$

implying the presence of combination overtones of the two basic frequencies ω_s and ω_f. We shall comment on the origin of this phenomenon in Sec. VI.

To accommodate this scheme in the general setting of Sec. II, one now needs four basic moments in terms of which all others can be expressed. Each of these closure relations

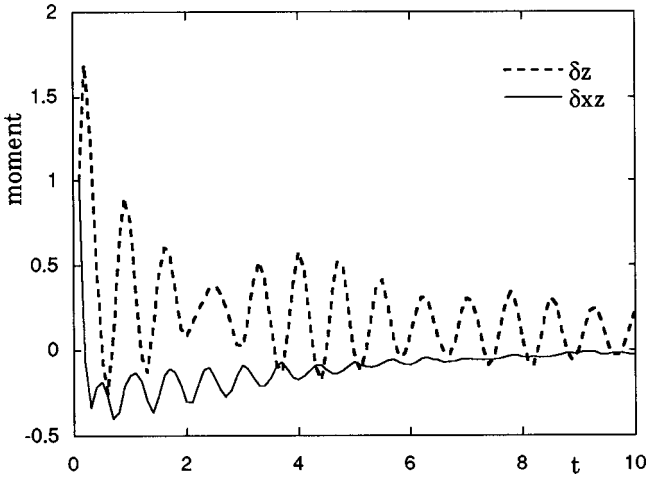

FIG. 6. Time evolution of the excess moments $\delta\overline{z}$ (broken line) and $\delta\overline{x\,z}$ (full line) normalized by their initial values in the case of the Lorenz model [Eqs. (32) with $r=28$, $\sigma=10$, and $b=\frac{8}{3}$] as obtained from 20 000 initial conditions uniformly distributed on the attractor.

will exhibit four phenomenological coefficients, whose values could be determined by a procedure similar to the one in Eqs. (29) and (30).

VI. CHAOTIC DYNAMICS IN THE PRESENCE OF SYMMETRIES

In this section we pursue the study of moment dynamics of chaotic systems by considering a different class of evolution equations admitting symmetries. The model on which the analysis will be illustrated is Lorenz's classical model [13]

$$\begin{aligned}\frac{dx}{dt}&=\sigma(-x+y),\\ \frac{dy}{dt}&=rx-y-xz,\\ \frac{dz}{dt}&=xy-bz\end{aligned}\tag{32}$$

for parameter values $r=28$, $\sigma=10$, and $b=\frac{8}{3}$.

One can check straightforwardly that these equations remain invariant under the transformation $(x,y,z)\rightarrow(-x,-y,z)$. As this invariance property will be shared by the Liouville operator $\hat{L}$ as well [Eq. (3)], we expect that there will be two classes of eigenfunctions of this operator which will be either even or odd in x and y. The first class will be the only one to contribute to the spectral representation [Eqs. (8) and (9)] of moments of the form $\overline{x^k y^{2m-k} z^l}$, and the second the only one to contribute to moments of the form $\overline{x^k y^{2m+1-k} z^l}$. In analogy with Sec. IV, we therefore expect even and odd moments associated with Eq. (32) to vary on the same scale within each class, and on different scales from one class to another. This is fully confirmed by simulation as illustrated in Fig. 6. The simulation reveals, in addition, that (a) odd moments vary on a faster scale than even ones; (b) odd moments vary monotonously in the long time limit; and (c) even moments execute damped composite oscillations in the long time limit, similar to those found in Sec. V. As a corollary of the above, closure relations are expected to hold only within each of these two classes of moments. In the sequel we analyze separately in some detail the case of even and odd moments.

A. Even moments

Owing to the composite character of the oscillations of the even moments revealed by Fig. 6, at least four different terms in the spectral representation of Eq. (9) are needed, corresponding to two pairs of complex conjugate eigenvalues with nearly identical real parts. A set of four equations involving only even excess moments can be deduced from Eq. (32) by straightforward manipulations. It reads

$$\begin{aligned}\frac{d}{dt}\,\delta\overline{x^2}&=-2\sigma\delta\overline{x^2}+2\sigma\delta\overline{x\,y},\\ \frac{d}{dt}\,\delta\overline{y^2}&=-2\delta\overline{y^2}+2r\delta\overline{x\,y}-2\delta\overline{x\,y\,z},\\ \frac{d}{dt}\,\delta\overline{z^2}&=-2b\delta\overline{z^2}+2\delta\overline{x\,y\,z},\\ \frac{d}{dt}\,\delta\overline{x\,y}&=r\delta\overline{x^2}+\sigma\delta\overline{y^2}-(\sigma+1)\delta\overline{x\,y}-\delta\overline{x^2z}.\end{aligned}\tag{33}$$

In the sequel we therefore consider $\overline{x^2}$, $\overline{y^2}$, $\overline{z^2}$, and $\overline{x\,y}$ as the basic set of even moments, and attempt to close the system of equations (33) by expressing $\overline{x\,y\,z}$ and $\overline{x^2z}$ as a linear combination of them [cf. Eq. (11)]:

$$\begin{aligned}\delta\overline{x\,y\,z}&=a_1\delta\overline{x^2}+a_2\delta\overline{y^2}+a_3\delta\overline{z^2}+a_4\delta\overline{x\,y},\\ \delta\overline{x^2z}&=b_1\delta\overline{x^2}+b_2\delta\overline{y^2}+b_3\delta\overline{z^2}+b_4\delta\overline{x\,y}.\end{aligned}\tag{34}$$

Substituting into Eq. (33), we obtain a closed linear system of equations for the four basic moments. The solutions of this system will display a behavior similar to Fig. 6 if the corresponding characteristic equation has two pairs of complex conjugate eigenvalues with similar real parts, and with imaginary parts related to the fast and slow oscillation frequencies or appropriate combination overtones as in Eq. (31). This, however, is not sufficient to determine all coefficients a_i and b_i. We therefore follow a different procedure: we require Eqs. (34) to hold at four different appropriately chosen times, compute numerically the instantaneous moments appearing in Eq. (34) for these four times, and deduce the coefficients a_i and b_i by solving the linear set of equations (34) for these unknowns. We then stipulate that the closure relations (34) should hold true for all times.

Figure 7 depicts the moments $\delta\overline{x^2z}$ and $\delta\overline{x\,y\,z}$ as obtained directly from the simulation (full lines) along with the values deduced from the closure relations (34) using the procedure explained above. The agreement is remarkably good, not only for the amplitude of the oscillations but for their phase as well, which as well known is a much more sensitive variable. Notice that this agreement is independent of the instantaneous values of the moments chosen to fit the parameters in Eqs. (34), provided that they are not too close. This result vindicates fully our closure ansatz. For reference we also give, in Fig. 8, a detailed plot of two typical even mo-

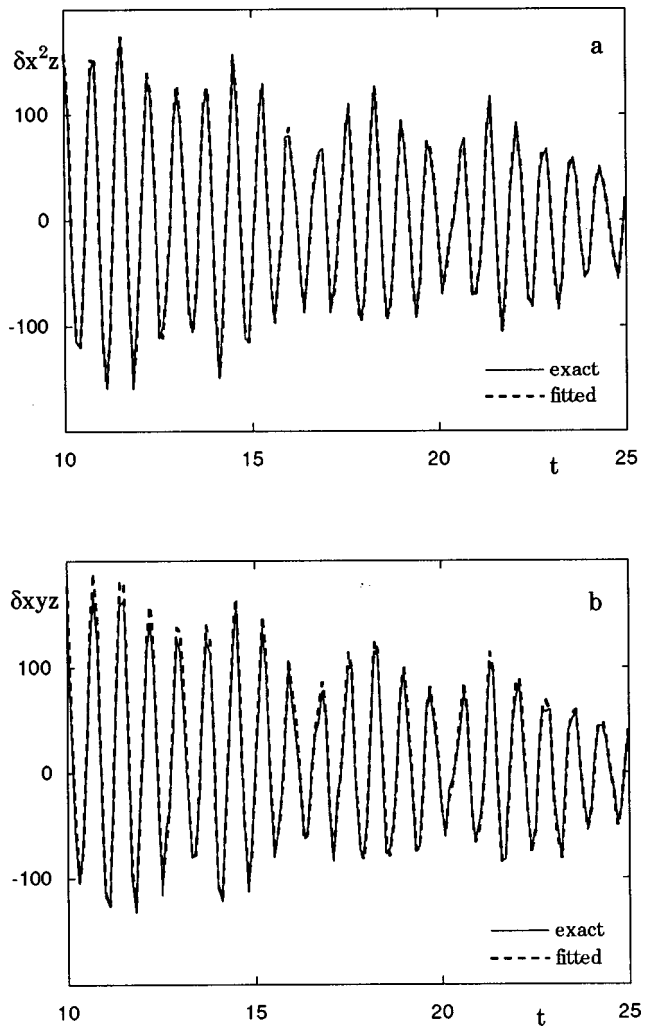

FIG. 7. Long time evolution of the excess even moments $\delta\overline{x^2 z}$ (a) and $\delta\overline{x\,y\,z}$ (b), obtained from simulation of system (32) (full lines) and from the closure relations (34) (broken lines). Parameters and initial conditions are as in Fig. 6.

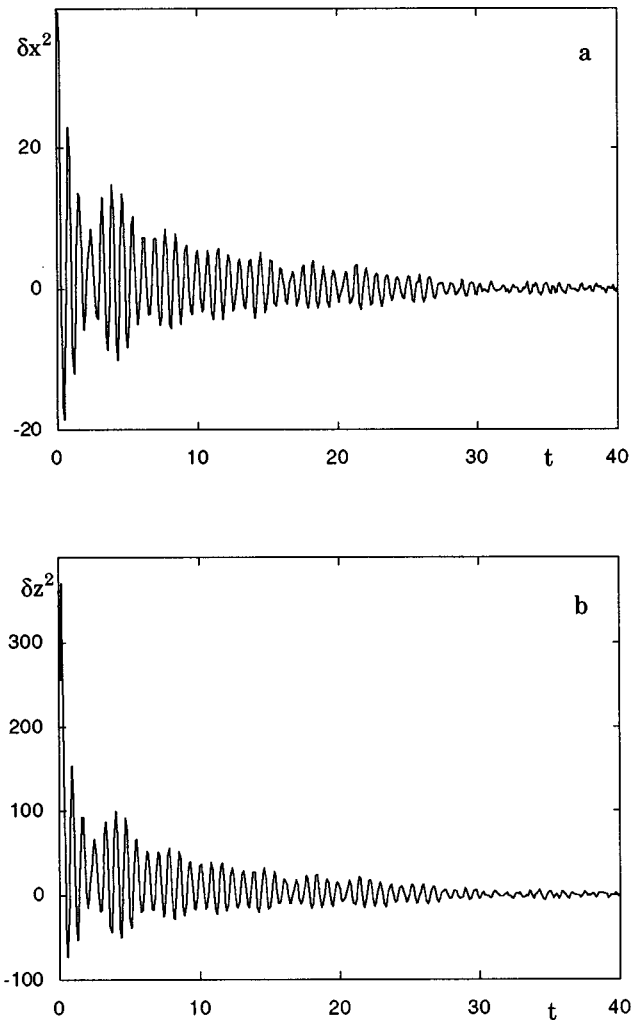

FIG. 8. Typical time evolution of the even excess moments $\delta\overline{x^2}$ (a) and $\delta\overline{z^2}$ (b). Parameters and initial conditions are as in Fig. 6.

ments $\delta\overline{x^2}$ and $\delta\overline{z^2}$, illustrating both the similarity in their behavior and the persistence of the composite oscillations during an extended lapse of time.

Having determined the values of a_i and b_i, one may come back to Eq. (33) and compute the roots of the characteristic equation. One indeed obtains two pairs of complex conjugate roots, whose imaginary parts are linear combinations of the fast and slow frequencies appearing in the figure, in much the same way as in Eq. (31).

We next comment on the origin of complex oscillations in the form of beatings observed in the transient behavior of the even moments of the Lorenz model, as well as of all moments of the Rössler model of Sec. V. The starting point is the connection between the eigenvalues of the Liouvillian and the zeros of the Selberg-Smale zeta function [14]

$$\zeta(\lambda)=\prod_p \sum_{k,l=0}^{\infty}\left(1-\frac{e^{-\lambda T_p}\lambda_p^l}{|\Lambda_p|\Lambda_p^k}\right)=0, \tag{35}$$

where the product is taken over all (unstable) periodic orbits contained in the chaotic attractor. T_p are the corresponding fundamental periods, and λ_p and Λ_p the contracting and the expanding eigenvalues on a Poincaré surface of section transversal to the cycle. These eigenvalues may be real or complex, positive or negative, provided that the inequalities $|\lambda_p|<1$, $|\Lambda_p|>1$ are satisfied.

A number of powerful techniques for carrying out such periodic orbit expansions explicitly has been reported [15] which, however, are typically applicable to hyperbolic systems. Much remains to be done for real-world fractal attractors such as the Rössler and Lorenz attractors. In the following we therefore limit ourselves to purely qualitative and somewhat speculative arguments. The main point is that in a chaotic attractor one expects strong interference effects between the successive unstable cycles. The first nontrivial instance in which such an interference will show up is when the infinite sum and product in Eq. (35) is truncated to its first two terms in which only the two shortest cycles having unstable eigenvalues closer to unity than any other cycle are retained. Setting $l=k=0$, expanding the product, and keeping only diagonal terms referring to these two cycles, from Eq. (35) one obtains

$$\frac{e^{-\lambda T_1}}{|\Lambda_1|}+\frac{e^{-\lambda T_2}}{|\Lambda_2|}=1. \tag{36}$$

If $|\Lambda_2|\gg 1$ the first term dominates in Eq. (36), and the corresponding eigenvalues are given by [16]

$$\lambda_n = \frac{2\pi i}{T_1} n - \frac{1}{T_1} \ln|\Lambda_1|, \quad n \text{ integer.} \tag{37}$$

At the level of the long time behavior of the moments, this would show up in the form of damped simple periodic oscillations, which is not the case in the present problem. It therefore seems reasonable to stipulate that the composite oscillations observed in Figs. 7 and 8 result from the joint effect of at least two unstable cycles on the underlying attractor of comparable (but different) expansion rates, $|\Lambda_1| < |\Lambda_2|$ and periodicities, $T_1 < T_2$. Equation (36) then becomes a transcendental equation whose solution will give, typically, combination overtones [17] of T_1 and T_2, just as observed in the simulation. Unfortunately the argument cannot be pushed to a more quantitative form, as T_i and $|\Lambda_i|$ are unknown for the models at hand.

B. Odd moments

We end this section by compiling the principal results concerning the analysis of the dynamics of odd moments of the Lorenz model. As seen from Fig. 6, these moments undergo a transient behavior in the form of an undershoot, followed by damped oscillations, and eventually a practically monotonous behavior in time. On the basis of this evidence we stipulate that two terms in the spectral representation of Eq. (9) should now be sufficient. A set of two equations involving only odd excess moments can be obtained from Eq. (32) by simply averaging the first two equations,

$$\begin{aligned} \frac{d\overline{x}}{dt} &= \sigma(-\overline{x} + \overline{y}), \\ \frac{d\overline{y}}{dt} &= r\overline{x} - \overline{y} - \overline{x\,y}. \end{aligned} \tag{38}$$

The corresponding closure relation replacing Eq. (34) is now expected to be

$$\delta\overline{x\,y} = a_1 \delta\overline{x} + a_2 \delta\overline{y}, \tag{39}$$

in which the coefficients a_1 and a_2 are to be determined by the same procedure as in Sec. VI A. Figure 9 summarizes the comparison between the ''exact'' time dependence of $\delta\overline{x\,z}$ obtained by direct simulation (full lines) and the ''fitted'' one using Eq. (39). The agreement is, again, remarkably good.

On replacing Eq. (39) into Eq. (38), one is in the position to obtain analytically the time dependence of $\overline{x}$ and $\overline{y}$ through the computation of the roots of the characteristic equation. The result is, again, consistent with the time dependencies obtained by direct simulation.

VII. CONCLUSIONS

We have proposed a simple algorithm for generating closure relations for the long time behavior of the moment equations of nonlinear dynamical systems. The method is applicable to a wide class of systems, provided that one accounts properly for symmetry properties and as long as there are finite gaps separating a set of ''dominant,'' slow eigenvalues from both the invariant eigenvalue and from the higher order ones.

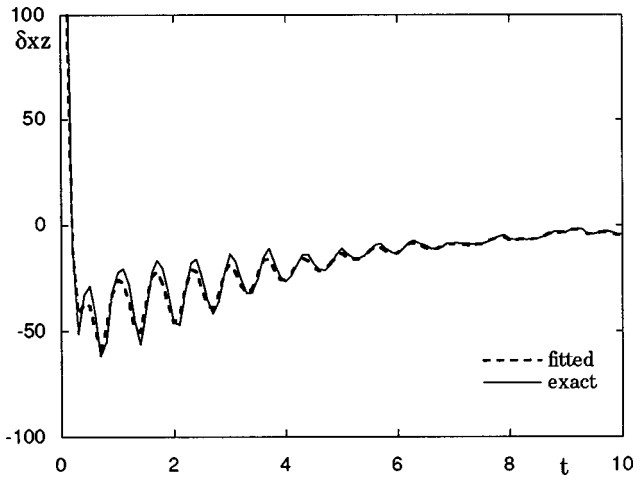

FIG. 9. Time evolution of the excess odd moment $\delta\overline{x\,z}$ as obtained from direct numerical simulation of system (32) (full line) and from the closure relation (39) (broken line). Parameters and initial conditions are as in Fig. 6.

The closure relations generated by our method bear strong similarities with the phenomenological relations linking the fluxes of irreversible processes to the associated generalized forces in irreversible thermodynamics. Well-known examples of such relations are Fourier's or Fick's laws, familiar in heat and mass transfer problems, and Stoke's law expressing momentum flux in terms of the velocity gradient in the Navier-Stokes equation. Common to all these relations is indeed that their origin lies in the spectral properties of the associated evolution operators. A major difference is, on the other hand, that the low-order moments in hydrodynamics may exhibit nontrivial time dependencies, including sustained oscillations or chaotic behavior, whereas the moment equations considered in the present work eventually admit a unique steady-state solution, as long as the system has strong ergodic properties. This is due to the nonexistence of conserved quantities in the class of dissipative dynamical systems considered in this study. The situation is likely to be different in spatially extended systems, which would undoubtedly be worth investigating in the future from this standpoint.

The nontrivial behavior of space averages in the long time limit has recently been established in systems of coupled map lattices, especially in the presence of global coupling [18]. Again, it would be interesting to study the moment dynamics of such systems in the framework of the approach outlined in the present paper, to assess whether such behavior finds its origin in the spectral properties of the evolution operator for the probability density replacing the Liouville operator for this class of systems.

ACKNOWLEDGMENTS

This research is supported by the Interuniversity Attraction Poles program of the Belgian Office for Scientific, Technical and Cultural Affairs, and by the Training and Mobility of Researchers program of the European Commission.

[1] N. Van Kampen, *Stochastic Processes in Physics and Chemistry* (North-Holland, Amsterdam, 1981).
[2] G. Nicolis, *Introduction to Nonlinear Science* (Cambridge University Press, Cambridge, 1995).
[3] A. Lasota and M. Mackey, *Probabilistic Properties of Deterministic Systems* (Cambridge University Press, Cambridge, 1985).
[4] C. Nicolis, Q. J. R. Meteorol. Soc. **118**, 553 (1992); C. Nicolis, S. Vannitsem, and J.-F. Royer, *ibid.* **121**, 705 (1995).
[5] J. Feder, *Fractals* (Plenum, New York, 1988).
[6] U. Frisch, *Turbulence* (Cambridge University Press, Cambridge, 1995).
[7] D. Schertzer, S. Lovejoy, F. Schmitt, Y. Chigirinskaya, and D. Marsan, Fractals **5**, 427 (1997).
[8] V. L'vov and I. Procaccia, Phys. Rev. E **53**, 3468 (1996).
[9] P. Gaspard, G. Nicolis, A. Provata, and S. Tasaki, Phys. Rev. E **51**, 74 (1995).
[10] H. Risken, *The Fokker-Planck Equation* (Springer, Berlin, 1984).
[11] O. Rössler, Ann. (N.Y.) Acad. Sci. **316**, 376 (1979).
[12] P. Gaspard and G. Nicolis, J. Stat. Phys. **31**, 499 (1983).
[13] E. Lorenz, J. Atmos. Sci. **20**, 130 (1963).
[14] S. Smale, *The Mathematics of Time* (Springer, Berlin, 1980).
[15] P. Cvitanovic, Physica D **51**, 138 (1991).
[16] G. Nicolis and P. Gaspard, Chaos Solitons Fractals **4**, 41 (1994).
[17] P. Gaspard and D. Alonso, Phys. Rev. A **45**, 8383 (1992).
[18] S. Morita, Phys. Lett. A **211**, 258 (1996).